ANALYSIS & VALIDATION OF MEAN VALUE MODELS FOR SI IC-ENGINES

C. SIVIERO*, R. SCATTOLINI*, A. GELMETTI*
L. POGGIO†, G. SERRA†

**Dipartimento Informatica e Sistemistica, Università di Pavia, 27100 Pavia, Italy. E-mail: siviero@ipvaimed3.unipv.it*
†Magneti Marelli, Divisione Controllo Motore, Sviluppo Sistema, 40134 Bologna, Italy. E-mail: LPoggio@bologna.maraut.it

Abstract. A Mean Value Model is developed for engine control design. The model structure is described by physical considerations and the model parameters are estimated from steady-state data obtained in cell tests on a FIAT engine. The proposed model is suitable for optimisation of engine control calibration.

Key Words. Modelling, Parameter estimation, Automobiles, Engine control.

1. INTRODUCTION

Mean Value Models (MVM) describe the dynamics of the main engine variables, measurable and unmeasurable, without considering cycle variations. These models are derived from a physical analysis of the main phenomena occurring inside the engine, while the model parameters are obtained by fitting. It is generally recognised that MVM have good predictive properties without being too complex. For this reason they are of particular interest in engine control (see e.g. Dobner, 1980; Aquino, 1981; Hendricks and Sorenson, 1990).

The aim of this paper is to present some preliminary results on the analysis and validation of a MVM applied to a FIAT engine. The model is constituted by two differential and a set of algebraic equations. These equations can be derived by physical considerations or by means of a "black-box approach" and contain a number of unknown parameters to be determined from experimental data.

2. SYMBOLS

$\dot{m}_{at}$	air mass flow rate past the throttle plate [Kg/sec];
$\dot{m}_f$	injected fuel mass flow [Kg/sec];
λ	relative air/fuel ratio;
p_{man}	intake manifold air pressure [Pa];
p_{amb}	ambient pressure [Pa];
p_{exh}	exhaust gas pressure [Pa];
p_{th}	pressure at the throat [Pa];
T_{man}	intake manifold air temperature [°K];
T_{amb}	ambient temperature [°K];
α	throttle plate angle [°];
α_0	throttle plate when tightly closed against the throttle bore [°];
A_{th}	throttle open area [m^2];
θ	spark advance angle [°];
η_b	brake thermal efficiency;
η_v	volumetric efficiency (based on intake conditions);
n	crank shaft speed [rpm];
I	total moment of inertia loading engine [$10^3(2\pi/60)^2$ Kgm^2];
T_b	brake torque [Nm];
P_b	brake power [KW];
H_u	fuel heating value [KJ/Kg];
V_d	engine displacement [m^3];
V	manifold-port passage volume [m^3];
r	compression ratio;
R	gas constant [J/Kg°K];
k	ratio of specific heats (C_p/C_v; 1.4 for the air);
C_f	flow coefficient of throttle body throat;
D	throttle bore diameter [m];
d	throttle shaft diameter [m];
M_a	inlet air molecular weight [g/mole];
M	working fluid molecular weight [g/mole];
HC	hydrocarbon emissions [g/KJ];
NO_x	nitric oxide emissions [g/KJ];
CO	carbon monoxide emissions [g/KJ].

3. EXPERIMENTAL SET-UP

To validate the engine model a set of about 450 steady-state measurements has been taken on a 1.6 litres, 16 valves FIAT 4 cylinder engine equipped with a Magneti Marelli multi-point injection system. The engine is mounted on an AVL PUMA4 /ISAC200 automatic dynamic test bench. This con-

trol system is equipped with an optical pick-up, giving a signal of 600 pulse/revolution from which the engine speed is derived, and controls the engine torque with a frequency of 14Hz. Throttle valve position and engine speed are controlled in closed-loop by a transputer which allows the reproduction of standard or arbitrary engine or vehicle test cycles, with an excellent control of engine speed and torque. To modify the engine control variables (e.g. θ and λ) the Engine Control Unit (ECU) has been coupled with an AVL-MCS3 (an EPROM emulator) system for remote control of all the ECU variables. The AVL-MCS3 is connected with the PUMA4; hence this system gives the possibility of acquiring simultaneously engine parameters and ECU variables too. Exhaust gases are measured by a five gases (CO_2, CO, NO_x, HC, O_2) analyser with an AVL730 fuel consumption equipment. The measurements have been conducted with λ control active (λ=1). The test bench keeps the engine operating point at fixed values of speed and torque during variation of spark advance, ranging from a minimum value of about 0 degree to a value of incipient knocking.

4. THE MEAN VALUE MODEL

4.1. Model description

Since in the performed cell tests the FIAT engine operated under λ control, the MVM here considered is constituted only by the two submodels describing the air mass flow in the intake manifold and the crank shaft speed dynamics, while the fuel film dynamics can be neglected.
Furthermore, some algebraic equations describe all the phenomena that exhaust in few motor cycles. Since the engine temperature is assumed to be at the steady-state, the model is not suitable to describe the warm-up phase.
The two differential equations are:

$$\dot{p}_{man} = -\frac{n}{120}\frac{V_d}{V}\eta_v p_{man} + \frac{RT_{man}}{V}\dot{m}_{at} \qquad (1)$$

$$\dot{n} = -\frac{P_b}{nI} + \frac{H_u \eta_b}{nI}\dot{m}_f \qquad (2)$$

The model is completed by a number of algebraic equations describing $\dot{m}_{at}$ as function of p_{th}, T_{amb} and α. Moreover, η_v and η_b depend on primary variables like n, θ, p_{man}. These dependencies have to be determined either by means of physical considerations or starting from a "black-box" approach based on a statistical analysis of data. Finally, the pollutants are assumed to depend, through some algebraic equations, on n, θ, λ, T_b. In these cases too a "black-box" modelling approach is adopted, since a significant physical description of the pollutants formation is complex and not necessary for the goals of the MVM here considered.

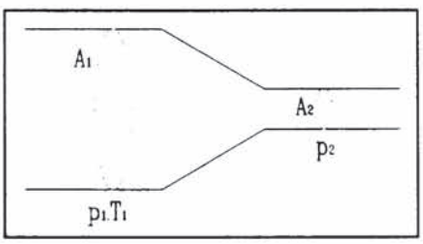

Fig. 1. Isentropic flow of a compressible gas in a pipe: symbols.

4.2. Model parameter estimation, complexity selection and validation

For simplicity the dependency of η_v, η_b, *HC, CO, NO* on the primary variables n, θ, λ, T_b, p_{man}, is assumed to be static. Furthermore physical considerations can be of great help in providing guidelines for the structural selection of these dependencies. However, the form of the functions to be estimated and their parameters have to be identified from data. To this regard, increasing the model complexity, that is the number of parameters to be estimated, in general leads to a more and more precise fitting of data. On the other hand, a natural requirement is to determine models with a limited number of parameters. Among the criteria for the model complexity selection presented in the literature, the Final Prediction Error (FPE) Criterion has been used in this work (see e.g. Söderström and Stoica, 1989). Then denoting by N the total number of data, by q the number of parameters to be estimated, by μ^2 the loss function, the FPE criterion consists of determining the model structure which minimises the following performance index:

$$FPE(q) = \frac{N+q}{N-q}\mu^2(q).$$

Moreover, a prediction error whiteness test (Söderström and Stoica, 1989) is performed to assess the prediction capability of the identified models.
For any given model structure, the parameter estimation procedure has been performed by minimising the mean square prediction error with different techniques, namely the Maximum Likelihood method and a Gauss Newton technique. The values of the parameters have been determined together with their relative standard deviation (r.s.d.). It has also been decided to reject models with estimated parameters characterised by a r.s.d. beyond 10%.

4.3. Air mass flow rate through the throttle plate

Air flow in a pipe. The air mass flow through the throttle plate can be viewed as a particular case of the isentropic flow of a compressible gas in a pipe. Under these assumptions, and with reference to the symbols of Fig. 1 , the air flow $\dot{m}$ through sections A_1 and A_2 with pressure p_1 and p_2 respectively, is given by:

$$\dot{m} = C_f \frac{p_1}{\sqrt{RT_1}} \frac{A_2}{\sqrt{1-\left(\frac{A_2}{A_1}\right)^2\left(\frac{p_2}{p_1}\right)^{2/k}}} \beta\left(\frac{p_2}{p_1}\right)$$

$$\text{for } \frac{p_2}{p_1} \geq r_{CR} = \left[\frac{2}{k+1}\right]^{k/k-1} \qquad (3.a)$$

$$\dot{m} = C_f \frac{p_1}{\sqrt{RT_1}} \frac{A_2}{\sqrt{1-\left(\frac{A_2}{A_1}\right)^2 (r_{CR})^{2/k}}} \beta(r_{CR})$$

$$\text{for } \frac{p_2}{p_1} \le r_{CR} \qquad (3.b)$$

where

$$\beta(x) = \sqrt{\frac{2k}{k-1}\left(x^{2/k} - x^{k+1/k}\right)} \qquad (3.c)$$

and C_f, nominally equal to 1, is to be determined experimentally in order to take into account structural defects or neglected physical factors (e.g. frictions). Furthermore, r_{CR} is the pression ratio which corresponds to the critical flow.

In particular, assuming that A_2 is the throttle plate open area A_{th} and section 1 in Fig. 1 is the ambient, so that $A_2/A_1=0$, expression (3) coincides with that given in Heywood (1988) and Hendricks (1990), with $p_2=p_{th}$, $p_1=p_{amb}$, $T_1=T_{amb}$.

Conventional throttle plates. In traditional throttle valves, an ellipsoidal throttle plate with throttle angle α is used, see Fig. 2.

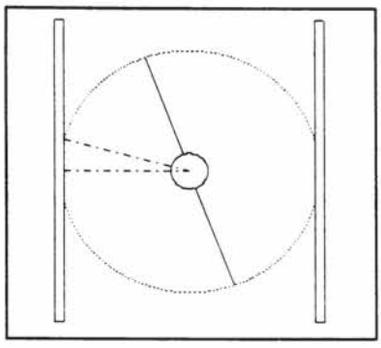

Fig. 2. A traditional throttle valve.

Letting $a=d/D$, A_{th} is given by:

$$\frac{4A_{th}}{D^2\pi} = \left(1-\frac{\cos\alpha}{\cos\alpha_0}\right) + \frac{2}{\pi}\left[\frac{a}{\cos\alpha}\left(\cos^2\alpha - a^2\cos^2\alpha_0\right)^{1/2} + \frac{\cos\alpha}{\cos\alpha_0}\sin^{-1}\left(a\frac{\cos\alpha_0}{\cos\alpha}\right) - a\left(1-a^2\right)^{1/2} - \sin^{-1}a\right]$$

$$\text{for } \alpha_0 \le \alpha \le \alpha^* \text{ where } \alpha^* = \cos^{-1}(a\cos\alpha_0) \qquad (4.a)$$

$$\frac{4A_{th}}{D^2\pi} = 1 - \frac{2}{\pi}\left[a\left(1-a^2\right)^{1/2} + \sin^{-1}a\right] \approx 1 - \frac{4d}{D\pi}$$

$$\text{for } \alpha^* \le \alpha \le \frac{\pi}{2} \qquad (4.b)$$

Expression (4) coincides with Eq. (7.18) in Heywood (1988), save for the sign of two terms.

Throttle valves with modified profile. In the last generation of throttle bodies, the internal profile is

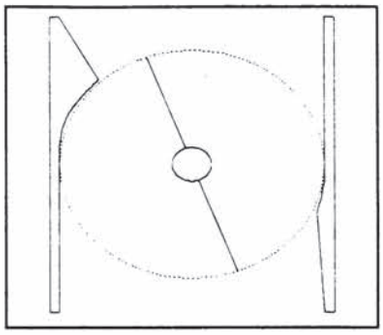

Fig. 3. Throttle valve with modified profile.

modified as shown in Fig. 3. This modified profile allows one to get some important benefits, such as the possibility to achieve better driveability characteristics through a much more precise control of the inlet air mass flow.

Indeed, for α less than a given angle, A_{th} grows almost linearly with α. In turn, thigh control of the air flow is a fundamental step in the development of efficient idle speed control techniques.

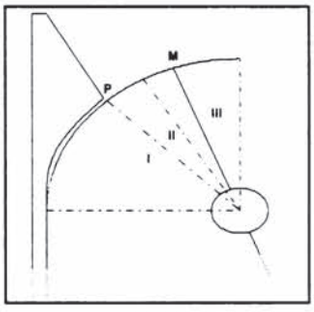

Fig. 4. Throttle open area calculus.

The computation of the area A_{th} is made difficult in view of the dissymmetry of the profile. In this work three different views corresponding to the three cases reported in Fig. 4 have been taken. In section I, A_{th} is computed as a function of α according to the view normal to the throttle plate. In section II, A_{th} is computed according to the view normal to the straight line between the edge of the plate (point M) and the modified profile (point P). Finally, in section III, the view is parallel to the straight line tangent to the throttle shaft and passing through the edge of the

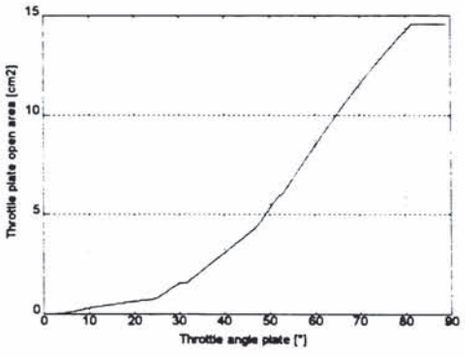

Fig. 5. Throttle plate open area versus throttle angle plate.

plate (point M).
With reference to the dimensions of the throttle body considered in this paper, the procedure above leads to compute the value of A_{th} reported in Fig. 5 as function of α. Note the substantial variation in the shape of A_{th} which occurs at about 24°.

Experimental results. Eq. (4) has been used together with the computed throttle plate open area of Fig. 5, to fit the data experimentally observed in the test cell for the FIAT engine. By considering in Eq. (4) C_f = 0.83, the results reported in Fig. 6 have been obtained. These results clearly illustrate that the adopted model provides excellent prediction capabilities for values of α<50° (the mean prediction error is about the 4.3%). On the contrary, for α>50° a significant departure of the predicted values of the air flow from the observed data is found. This can be explained as follows: in Eq. (3) p_2 should coincide with p_{th}, while in the performed experiments p_{man} has been used. Since $p_{man} > p_{th}$, an error is introduced which can be only partially corrected by the selection of C_f. In fact, the shape of $\beta(p_{man})$ is found to be constant up to critical flow; then in this region, which corresponds to small values of α, the use of p_{man} instead of p_{th} does not lead to any error. On the contrary, for high values of α, an error in the pressure measure induces through $\beta(p_{man})$ a significant error in the computed air mass flow rate. In view of these considerations better results in all the operating range could only be achieved by modifying the pressure sensor position in the manifold.

4.4. The volumetric efficiency

Many models for the volumetric efficiency η_v have been proposed in the literature. A "black-box" approach has been adopted in Hendricks and Sorenson (1990) where the dependence of η_v upon n and p_{man} is assumed to be given by the following model:

$$\eta_v = \eta_{vn0} + \eta_{vn1}\, n + \eta_{vn2}\, n^2 + \eta_{vp1}\, p_{man}. \qquad (5)$$

By means of the maximum likelihood technique, the unknown parameters of (5) have been estimated together with their r.s.d., leading to: η_{vn0} = 0.133 (r.s.d. = 29.9 %), η_{vn1} = 0.391e-3 (r.s.d. = 8.2 %), η_{vn2} = -0.0636e-6 (r.s.d. = 9.3 %) and η_{vp1} = 0.202e-5 (r.s.d. = 9.8 %). Note that, although the model has good prediction capabilities, the estimated parameters have unacceptable r.s.d..

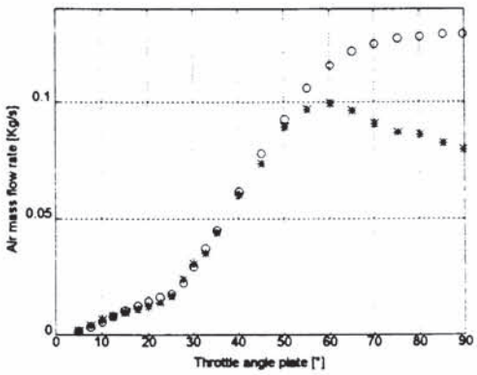

Fig. 6. Air mass flow rate through the throttle valve measured (o) and predicted (*) as functions of α.

A second approach is to determine η_v by means of physical considerations. To this end, Heywood (1988) presents the following relation:

$$\eta_v = \frac{M}{M_a}\frac{1}{1+\frac{1}{14.7\lambda}}\left[\frac{r}{r-1} - \frac{1}{k(r-1)}\left(\frac{p_{exh}}{p_{man}} + (k-1)\right)\right] \qquad (6)$$

It is worth noting that, for a wide range of λ

$$\frac{M}{M_a}\frac{1}{1+\frac{1}{14.7\lambda}} \approx 1.$$

Then Eq. (6) reduces to

$$\eta_v = \frac{r}{r-1} - \frac{1}{k(r-1)}\left(\frac{p_{exh}}{p_{man}} + (k-1)\right) \qquad (7)$$

which is the form given in Taylor (1977), Boam *et al.*, Matthews *et al.* (1991). According to (7), the physical model we have adopted takes the form:

$$\eta_v = c\left[\frac{r}{r-1} - \frac{1}{k(r-1)}\left(\frac{p_{exh}}{p_{man}} + (k-1)\right)\right] \qquad (8)$$

The identification procedure leads to c=0.86 with r.s.d. 0.31%, while the prediction capabilities of the model are equivalent to those of model (5).

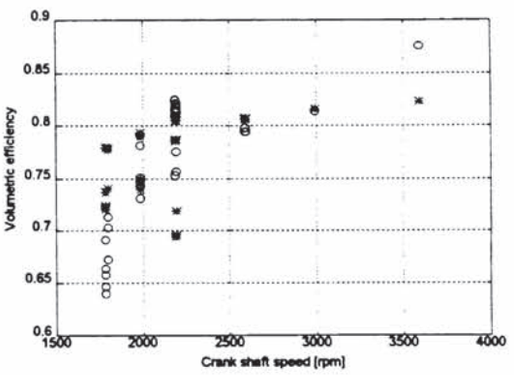

Fig. 7. Values of η_v measured (o), and predicted (*) by the model (8), as functions of n.

Note however that model is characterised by a single parameter, whose value can be estimated with great accuracy. The experimental data (o) are compared to the predicted ones (*) in Fig. 7. A prediction error whiteness test has also been performed to assess the model accuracy. This test has shown a significant bias with respect to n. A possible interpretation is that Eq. (7) takes into account quasi-static effects only, while dynamic effects are neglected. Among these, the reverse flow can be significant at low values of n, while resonance and wave effects can increase the value of η_v at high engine speed. For these reasons it has been considered a different model of the form:

$$\eta_v = c_1\left[\frac{r}{r-1} - \frac{1}{k(r-1)}\left(\frac{p_{exh}}{p_{man}} + (k-1)\right)\right] + c_2 n^2 \qquad (9)$$

The estimation procedure has been repeated for two different sets of data. In the first data set only experimental data with n<2400 rpm have been used to determine c_1 = 0.55 (r.s.d. 1%) and c_2 = 64.84e-9 (r.s.d. 1.8%). In the second one, data corresponding to n>2400 lead to estimate c_1 = 0.76 (r.s.d. 0.6%) and c_2 = 11.2e-9 (r.s.d. 3.9%) . This model is characterised by a very low prediction error and excellent r. s.d. of the estimated parameters. Experimental (o) and predicted data (*) are reported in Fig. 8.

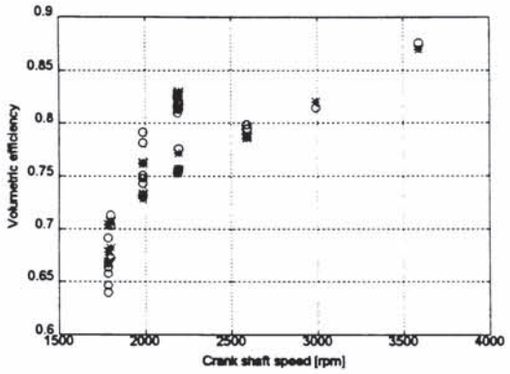

Fig. 8. Values of η_v measured (o) and predicted (*) by the model (9), as functions of n.

4.5. The brake thermal efficiency

In the literature, η_b is usually represented as a "black-box" function of n, λ, θ, p_{man}. However, being the FIAT engine only weakly sensitive to variations in θ, a physical model for η_b has been derived as follows. From the speed-density law one gets:

$$\dot{m}_f = \frac{V_d}{120.R}\frac{n.p_{man}.\eta_v}{T_{man}.(\lambda 14.7)} \qquad (10)$$

On substituting this expression in (2) and by recalling the form of η_v (7), at the steady-state it results:

$$\eta_b = c_0\frac{T_b.T_{man}.\lambda}{p_{man} + c_1 p_{exh}}. \qquad (11)$$

The unknown parameters of model (11) have been estimated as follows: c_0 = 0.8101 (r.s.d. 0.9 %) and c_1 = -0.0861 (r.s.d 4.2 %).

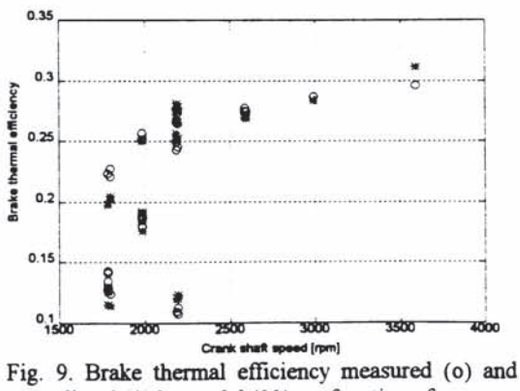

Fig. 9. Brake thermal efficiency measured (o) and predicted (*) by model (11), as function of n.

With reference to this model, the predicted values of η_b (*) are compared to the measured ones (o) in Fig. 9, as functions of n.

4.6. The brake torque

A criticism which could be made to the model here presented is due to the dependence of some quantities *(η_v, η_b, HC, NO, CO)* upon p_{exh} and T_b, while for control design purposes, it could be undoubtedly better to describe them as functions of the state variables n, p_{man} or the manipulated variables λ an θ. As for p_{exh}, experimental evaluation has shown that taking constant its value produces only a slight degradation of the performance of models (9) and (11). Things are more involved for T_b; however, it has to be recalled here that, in the near future, the measure of T_b will be available at low costs. Moreover, it is also possible to follow a black box approach where

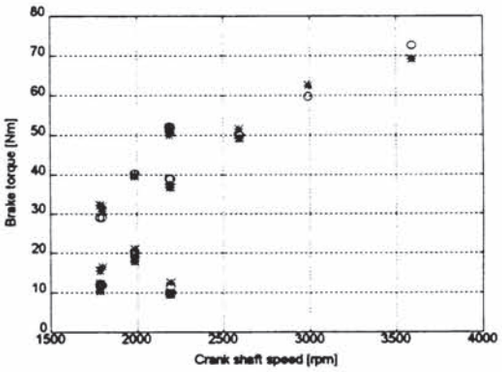

Fig. 10. Values of T_b measured (o) and predicted (*) by (12), as functions of n.

T_b is estimated from n, p_{man}, λ, θ. For example, the following regression model has been considered:

$$T_b = c_0 + c_1.n + c_2.\, n\theta + c_3.\theta \qquad (12)$$

which leads to the results of Fig. 10, with c_0 = 0.16e-2 (r.s.d. 1%), c_1 = -2.15e-2 (r.s.d. 2.7%), c_2 = -1.9 (r.s.d. 1.4%) and c_3 = 0.1e-2 (2.2%).

4.7. Exhaust emissions models

The physical phenomena producing *HC, CO, NO_x* are clearly and extensively illustrated in Heywood (1988), and in the references there reported. However, being these phenomena highly involved, a common approach in the literature, see e.g. Tennant *et al.* (1983) and Pianese and Rizzo (1992), is to determine empirical (static) relations of these pollutants with engine variables; the unknown parameters of these models can then be estimated as described in Paragraph 4.2. This procedure leads to more tractable models suitable for control. Since the FIAT engine operated under λ control, another set of data obtained from tests on an ALFA ROMEO Boxer engine was used to select the model structures. Then, these models were validated also on the FIAT en-

gine. For space limitations, the results concerning the Boxer engine are not reported here.

Hydrocarbon emission. The model structure selected takes the form:

$$HC=c+\lambda_1\lambda+\lambda_2\lambda^2+\theta_1\theta+T_{b1}T_b \qquad (13)$$

With respect to previous results (Tennant *et al.*, 1983) no significant dependence of *HC* upon *n* was found. The estimated parameters for the FIAT engine (recall that λ=1) are: c=0.128e-2 (r.s.d. 7.6%), θ_1=0.52e-4 (r.s.d. 5.9%), T_{b1}=-0.2e-4 (r.s.d. 3.8%). In order to illustrate the performance of this model, in Fig. 11 a number of collected (o) and predicted (*) data are reported as function of θ.

Nitric Oxide. According to Heywood (1988), the engine variables which mainly influence *NO* emissions are λ and θ. Furthermore, the performed analysis has shown a dependence on T_b. This dependence has also been experimentally found in Tennant *et al.* (1983). Roughly the dependence of *NO* upon λ can be interpreted as quadratic, while in a wide range (about $10°\leq\theta\leq40°$) *NO* grows linearly with θ. This justifies that the best model structure, among the considered ones, takes the form:

$$NO=c+\lambda_1\lambda+\lambda_2\lambda^2+\theta_1\theta+T_{b1}T_b \qquad (14)$$

The estimated parameters are: c=-.26e-2 (r.s.d. 10.9%), θ_1=0.13e-4 (r.s.d. 6.9%), T_{b1}=0.91e-4 (r.s.d. 2.5%).

Carbon monoxide. It is well known that the production of *CO* mainly depends on λ; in the analysis a quite weak but statistically significant dependence on T_b has been found; then, the model here adopted is:

$$CO = e^{-\lambda/\lambda_1}\left(T_{b0}+T_{b1}T_b\right) \qquad (15)$$

The estimated model parameters are: T_{b0}=0.23e-1 (r.s.d. 1.9%). T_{b1}=-0.2e-3 (r.s.d. 5.1%).

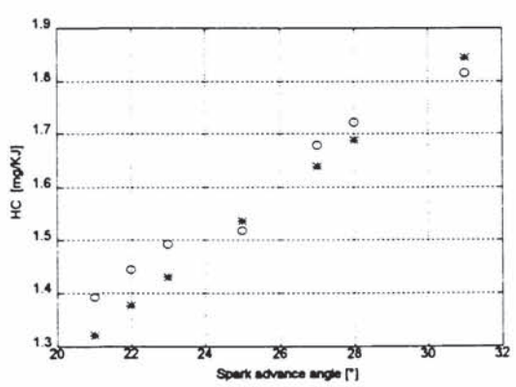

Fig. 11. *HC* emissions of the Fiat engine measured (o) and predicted (*), as functions of θ.

5. CONCLUSIONS

In this paper a MVM for spark ignition engines has been presented and validated. Future work is aimed at verifying the predictive capabilities of the model in dynamic conditions. Moreover, the film fluid phenomenon can be included together with the dependencies of the model on the intake manifold and the cylinder wall temperatures in order to cope with the warm-up phase.

Acknowledgements. The authors gratefully acknowledge the help of Prof. G. Rizzo and Ing. C. Pianese in providing the data of the ALFA ROMEO Boxer engine.

6. REFERENCES

Aquino, C.F. (1981). Transient A/F Control Characteristics of the 5 Litre Central Fuel Injection Engine. *SAE Paper 810494*.

Boam, D.J., I.C. Finlay and J.J.G. Martins (1989). A Model for Predicting Engine Torque Response during Rapid Throttle Transients in Port-injected Spark Ignition Engines. *SAE Paper 890565*.

Dobner, D.J. (1980). A Mathematical Engine Model for Development of Dynamic Engine Control. *SAE Paper 800054*.

Hendricks, E. and S.C. Sorenson (1990). Mean Value Modelling of Spark Ignition Engines. *SAE Paper 900616*.

Heywood, J.B. (1988). *Internal Combustion Engine Fundamental*. McGraw-Hill, New York.

Matthews, R.D., S.K. Dongre and J.J. Beaman (1991). Intake and ECM Submodel Improvements for Dynamic SI Engine Models: Examination of Tip-IN/Tip-Out. *SAE Paper 910074*.

Pianese, C. and G. Rizzo (1992). A Dynamic Model for Control Strategy Optimisation in Spark Ignition Engines. *Proc. of Third ASME Symp. on Trasp. System*, **44**, 253-267.

Söderström, T. and P. Stoica (1989). *System Identification*. Prantice Hall, Cambridge.

Taylor, C.F. (1977). *The Internal-Combustion Engine in Theory and Practice*. The MIT Press, Cambridge.

Tennant, J.A., A.I. Cohen, H.S. Rao and J.D. Powell (1983). Computer-aided procedures for optimisation of engine controls. In: *Application of Control Theory in the Automotive Industry* (R. Fruechte, Ed.), pp. 1-12. Inderscience Enterprises Ltd., Genève.